Marine Micropaleontology 141 (2018) 10–22

Contents lists available at ScienceDirect

Marine Micropaleontology

journal homepage: www.elsevier.com/locate/marmicro

Research paper

Late Holocene oceanographic and climatic variability recorded by the Perseverance Drift, northwestern Weddell Sea, based on benthic foraminifera and diatoms

Anastasia Kyrmanidou[a,*], Kara J. Vadman[b,c], Scott E. Ishman[a], Amy Leventer[b], Stefanie Brachfeld[d], Eugene W. Domack[c,e,1], Julia S. Wellner[f]

[a] Department of Geology, Southern Illinois University, Carbondale, IL 62901-4324, USA
[b] Department of Geology, Colgate University, Hamilton, NY 13346, USA
[c] College of Marine Science, University of South Florida, St. Petersburg, FL 33901, USA
[d] Department of Earth and Environmental Studies, Montclair State University, Montclair, NJ 07043, USA
[e] Department of Geosciences, Hamilton College, Clinton, NY 13346, USA
[f] Department of Earth and Atmospheric Sciences, University of Houston, TX 77204, USA

ARTICLE INFO

Keywords:
Foraminifera
Diatoms
Holocene
Weddell Sea
Antarctica

ABSTRACT

The Perseverance Drift, located in the Joinville-D' Urville Trough, northwestern Weddell Sea, records changes in ocean and sea ice conditions throughout the middle to late Holocene, with a record extending back to ca. 3400 yr BP. The 2562-cm composite record collected from a water depth of 806 m, documents the uppermost section of the 90-m thick sediment drift. Spring-blooming diatoms (*Chaetoceros* subg. *Hyalochaete*) are abundant through the sedimentary record. The greater proportion of *Chaetoceros* vegetative valves compared to resting spores indicates that the marine environment is highly productive, and nutrients generally are not limiting. Epiphytic diatoms, dominated by *Cocconeis* spp., are observed throughout JKC36, suggesting transport of algal detritus from shallower regions to the benthos. Three foraminiferal assemblages (FAs): *Miliammina* spp., *Globocassidulina* spp., and *Paratrochammina bartami/Paratrochammina lepida/Portatrochammina antarctica* characterize the benthic foraminiferal fauna and reflect affinities with water masses circulating across the Perseverance Drift and tolerance to corrosive bottom waters. The interval 3400–1800 yr BP is marked by high abundances of *Globocassidulina* spp., indicating incursions of Weddell Sea Transitional Water over the drift site. This interval implies a period of "freshening" of the water column, coinciding with an open-marine or seasonally open-marine environment during the middle-to-late Holocene Climatic Optimum. The interval 1800 yr BP to the present displays characteristics of slightly colder conditions, as indicated by the absence of the calcareous *Globocassidulina* spp. FA, and the pronounced presence of agglutinated *P. bartami/P. lepida/P. antarctica* FA, along with other agglutinated species that are indicative of the presence of sea ice. Therefore, this interval is interpreted to represent the onset of Neoglaciation at the northeastern tip of the Antarctic Peninsula. The consistent presence of *Miliammina* spp. FA corroborates that the sedimentary record represents a productive, open-marine setting with seasonally variable sea ice extent. The Drift is a unique geologic archive that provides an excellent target for future coring based on the preservation of abundant carbonate material for radiocarbon dating and the potential to develop a multi-proxy data set that could offer a robust understanding of the Holocene depositional and paleoclimatic conditions of the northwestern Weddell Sea.

1. Introduction

The Antarctic Peninsula (AP) is an area of Recent Rapid Regional (RRR) warming where the regional changes in atmospheric temperatures exceed the global mean (Vaughan et al., 2003; Cook et al., 2005). In the last 50 years, surface air temperatures at several research stations in the AP have shown significant rises, such as +3.71 °C at Argentina's Matienzo Station between 1962 and 1972 and 1999–2010 (Cape et al., 2015). The AP warming has been coincident with an array of environmental changes. During the last several decades for example,

* Corresponding author at: Department of Geology, Southern Illinois University, 1259 Lincoln Dr, IL 62901-4324, USA.
E-mail address: akyrmanidou@siu.edu (A. Kyrmanidou).
[1] Deceased 11/20/2017.

https://doi.org/10.1016/j.marmicro.2018.03.001
Received 27 July 2017; Received in revised form 5 March 2018; Accepted 18 March 2018
Available online 29 March 2018
0377-8398/

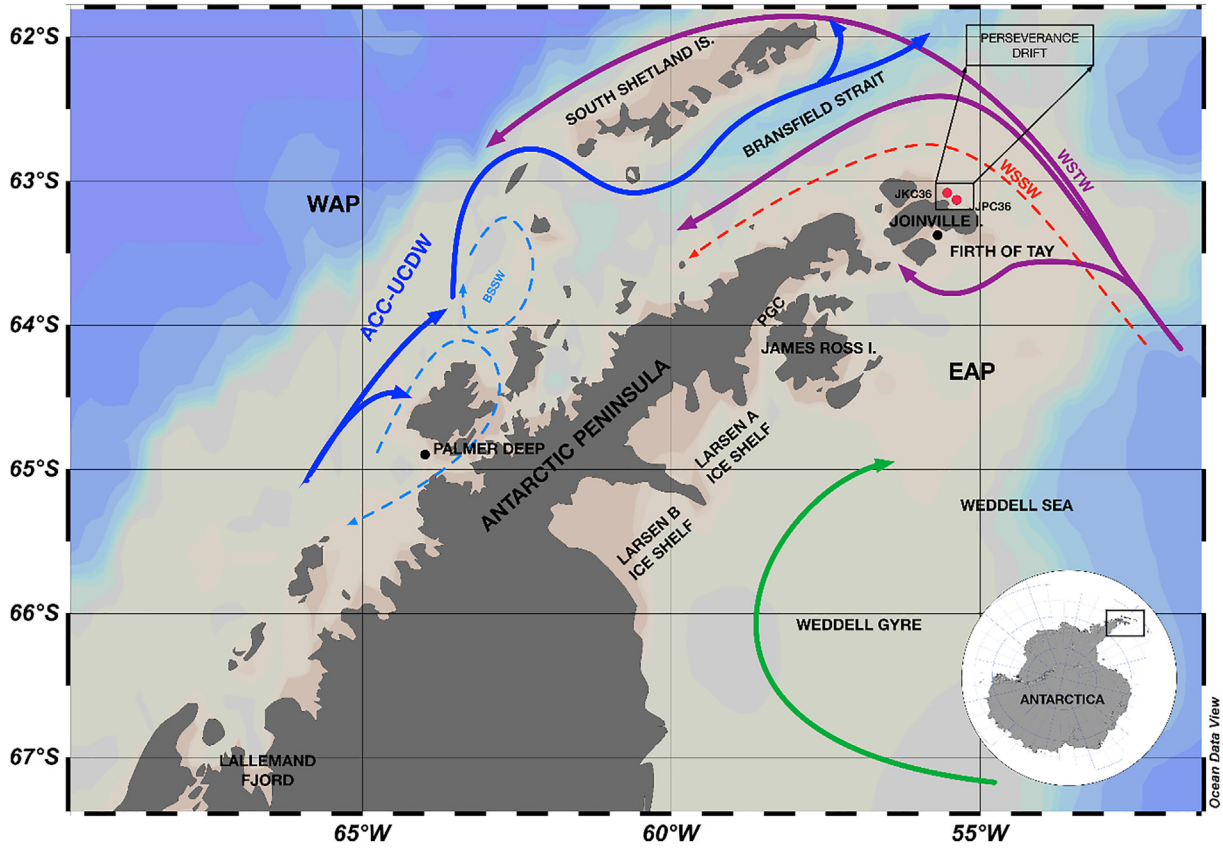

Fig. 1. Map of the northern Antarctic Peninsula showing the Perseverance Drift core sites JPC36 and JKC36 (generated with Ocean Data View, http: http://odv.awi.de/). Regional deep water circulation is indicated by solid lines and surface water circulation by dashed lines. Arrows show general flow circulation (modified from Ishman and Domack, 1994; Shevenell and Kennett, 2002). ACC: Antarctic Circumpolar Current; UCDW: Upper Circumpolar Deep Water; BSSW: Bransfield Sea Surface Water; WSTW: Weddell Sea Transitional Water; WSSW: Weddell Sea Surface Water. Inset image shows the location of the Antarctic Peninsula in a mosaic of Antarctica (modified from the National Snow and Ice Data Center, http://nsidc.org/). Study sites with published records are shown: Lallemand Fjord (Shevenell et al., 1996; Domack et al., 2003), Palmer Deep (Domack et al., 2001; Ishman and Sperling, 2002), Larsen A (Brachfeld et al., 2003), PGC: Prince Gustav Channel (Pudsey and Evans, 2001; Pudsey et al., 2006), James Ross Island (Björck et al., 1996); Firth of Tay (Majewski and Anderson, 2009; Michalchuk et al., 2009).

satellite data indicate shortening of the sea ice season in most of the AP and Bellingshausen Sea regions (Stammerjohn et al., 2012), consistent with the negative trend in sea ice extent (1978–2010) of $-8200 \pm 1200\,km^2\,yr^{-1}$ in the Bellingshausen and Amundsen Seas (Parkinson and Cavalieri, 2012), and a 4–10% per decade decrease in sea ice concentration in the Bellingshausen and western Weddell Sea sectors between 1979 and 2002 (Liu et al., 2004). Moreover, hydrographic data indicate that ocean temperature warming affects not only upper- (Reynolds and Smith, 1994) and mid-depths in the Southern Ocean (Gille, 2002), but also deeper waters of the Weddell Sea (Robertson et al., 2002). Reduced salinification (0.09) of the northwestern Weddell Sea continental shelf (1989–2006) has also been measured (Hellmer et al., 2011), while model simulations predict a decrease in ventilation of deep convective regions in the Weddell Sea, and even cessation of convection under a climate scenario attributable to freshwater input (De Lavergne et al., 2014).

Cryosphere changes also include destabilization of floating ice shelves, which have responded rapidly to climate warming in the AP. Ice shelves in the northwestern Weddell Sea (Prince Gustav Channel, Larsen Inlet, Larsen A, Larsen B) and along the western Antarctic Peninsula have retreated during the time of historical observations and during the modern era of instrumental measurements (Vaughan and Doake, 1996; Skvarca et al., 1999; Cook and Vaughan, 2010). Both of the large-scale, rapid disintegration events of the Larsen Ice Shelf System in 1995 (Larsen A) and 2002 (Larsen B) occurred during record warm air temperatures (Rott et al., 2002; Scambos et al., 2004). The disintegration of ice shelves has increased the discharge of grounded ice from glaciers to the ocean (Rignot et al., 2004; Scambos et al., 2004). In fact, 87% of the glaciers that feed the AP ice shelves have retreating fronts (Cook et al., 2005) with a clear southerly migration of the boundary between the mean advance and mean retreat, which is consistent with the southward migration of the mean annual AP isotherm positions, and in line with the regional atmospheric warming trend (Morris and Vaughan, 2003).

Many high quality paleoenvironmental records have been constructed to decipher the temporal and spatial patterns of climate change on both sides of the AP region during the Holocene. A review by Bentley et al. (2009) provides a synthesis of these proxy records and the conclusions drawn from them. These studies document distinct periods of significant warming and cooling, reveal differences between the response of marine and terrestrial systems to climate forcing, as well as differences between the east and west sides of the AP, all of which suggests asynchronicity in the duration and magnitude of Holocene climatic events (Bentley et al., 2009).

The unprecedented recent atmospheric warming and the documented Holocene climatic variability of the AP underscore the importance for further investigating the timing, magnitude, underlying mechanisms, and geographic extent of the changing cryosphere in the AP throughout the Holocene. Analysis of high-quality marine paleoclimatic records from the AP contributes to the understanding of past ice behavior, and these records provide analogs for future climatic shifts.

This study targets the history of northeastern AP water masses via analysis of benthic foraminifera and diatom microfossil assemblages

from the Perseverance Drift, located in the northwestern Weddell Sea. These data are used to reconstruct a late Holocene record of environmental and oceanographic conditions present at the tip of the AP where cold Weddell Sea Transitional Water (WSTW) branches off the Weddell Sea Gyre and flows through the Bransfield Strait en route to the western AP.

2. Regional setting

2.1. General oceanography of the Weddell Sea

The AP is a narrow, rugged spine of glaciated mountains that extend 1250 km north from the continent between 62 and 75°S latitude and 55–80°W longitude (Fig. 1). The AP region also includes the South Shetland Islands and the islands immediately east and northeast of the Trinity Peninsula (Domack et al., 2003; Ingólfsson et al., 2003). The AP is a boundary that creates distinct climatic zones on its western and eastern sides (Domack et al., 2003). The western AP is characterized by warmer maritime conditions generated by the southern westerly winds, which carry warm, moist air masses derived from mid-latitudes. The western AP is influenced by the Antarctic Circumpolar Current (ACC), which transfers relatively warm and saline Circumpolar Deep Water (CDW) onto the continental shelf (Martinson and McKee, 2012; Smith and Klinck, 2002). The eastern side of the AP experiences a colder and drier climate, influenced by the northward extension of cold continental winds derived from the Antarctic interior.

The circulation of the Weddell Sea is influenced mainly by the Weddell Sea Gyre, located south of the ACC (Gill, 1973; Orsi et al., 1993). The eastern limb of the gyre entrains and transfers warm Upper Circumpolar Deep Water (UCDW) southward to the inner Weddell Sea, where it is modified to slightly cooler Warm Deep Water (WDW), also known as Weddell Deep Water (Carmack, 1974). This water mass is carried to the north in the western limb of the gyre, which also transports sea ice to the northwestern Weddell Sea, where a branch then flows southwest into the Bransfield Strait in the form WSTW (Orsi et al., 1993; Fahrbach et al., 1995, 2001).

2.2. Perseverance drift study area

Perseverance Drift (PD) is located in the Joinville-D' Urville Trough, immediately north of Joinville Island, and contains up to 90 m of Holocene sediment. Mutlibeam data have indicated that during the Last Glacial Maximum (LGM), ice was grounded on the Joinville Plateau, located east of the Joinville Island, suggesting that the Antarctic Peninsula Ice Sheet (APIS) extended across the continental shelf. During the subsequent deglaciation, the grounded ice began to retreat while shedding sediments onto the continental shelf (Lavoie et al., 2015). Perseverance Drift was sampled during NBP12–03, when a 5.19 m kasten core and a 23.82 m jumbo piston core were both obtained from a sea bed depth of 806 m. The two core sites are approximately 600 m apart (Fig. 1). The study area between Joinville and D' Urville Islands is ideally located to record oceanographic variability from the influence of WSTW. Cold and saline WSTW flows north out of the Weddell Sea and then west and south through the Bransfield Strait, where it meets and interacts with upwelled UCDW (Tokarczyk, 1987; Ishman and Domack, 1994; Shevenell and Kennett, 2002). A permanent pycnocline, whose characteristics vary seasonally with the intensity of sea ice formation and meltwater production, separates these relatively warm, intermediate waters from the colder Weddell Sea Surface Waters (WSSW) and shelf waters (Foster and Carmack, 1976) that flow around the Joinville and D' Urville Trough.

2.3. Studies on benthic foraminifera from the AP

Foraminifera have been collected in Antarctic waters since the first half of the 19th century (Gooday et al., 2003). Antarctic foraminiferal faunas include calcareous and agglutinated forms. They are organic-cemented (with the exception of the genus *Miliammina* which is siliceous), and according to the environmental setting in which they occur, assemblages can be characterized by benthic-agglutinated, benthic-calcareous, and calcareous-planktonic taxa. Benthic foraminifera distributions are amongst the most sensitive indictors of paleoceanographic and paleoclimatic conditions because they are influenced by subtle differences in sediment type, bottom current transport, organic matter content, bathymetry, salinity, sea ice extent, and water mass characteristics (Anderson, 1975a,b; Milam and Anderson, 1981; Ishman and Domack, 1994; Murray, 2001; Gooday et al., 2003; Ishman and Szymcek, 2003; Jorissen et al., 2007; Majewski and Anderson, 2009).

In complex environmental settings that are characterized by seasonal or perennial ice cover, such as the Weddell Sea continental shelves and slopes, the ecology and distribution patterns of benthic foraminifera follow that of major water masses surrounding the continental margin, and have been useful as glacial and paleoceanographic indicators in various studies (Anderson, 1972, 1975a,b; Mackensen et al., 1990; Ishman and Sperling, 2002). Specifically, Anderson (1975a,b) emphasized the control sea ice extent exerts on the factors responsible for the distribution of modern species, with the observation that the carbonate compensation depth (CCD) and foraminiferal lysocline in the Weddell Sea is related to water-mass more so than water-depth. This conclusion is supported by the contrasting foraminiferal faunas encountered in the eastern and southwestern Weddell Sea continental shelf regions. The eastern part, which is associated with the circulation of Fresh Shelf Water, is inhabited primarily by calcareous forms, whereas the southwestern continental shelf, which is perennially ice-covered and associated with the circulation of Saline Shelf Water, is inhabited predominantly by agglutinated forms. For Saline Shelf Water, high salinity values promote CO_2 concentration underneath the sea ice pack, which suppresses the precipitation and preservation of carbonate material (Anderson, 1975a,b).

2.4. Studies on modern diatoms from the AP

Diatoms dominate the phytoplankton community in the Southern Ocean. They possess silica tests that are typically well preserved in Southern Ocean sediments. They are of particular geologic importance because they exhibit diverse habitat preferences that record past environmental conditions (Leventer, 1998; Armand et al., 2005, 2017). Studies from the AP document the role of seasonal duration of sea ice cover, water column stratification and nutrients in controlling diatom distribution (for example, Leventer, 1991; Buffen et al., 2007; Pike et al., 2008; Swilo et al., 2016). On the eastern side of the AP, Buffen et al. (2007) presented a study of surface sediment diatom assemblages in relation to present oceanographic conditions. Their data identified a sea ice associated assemblage dominated by *Fragilariopsis curta*, with contributions from other less common *Fragilariopsis*, such as *Fragilariopsis cylindrus*, *Fragilariopsis sublinearis* and *Fragilariopsis vanheurckii*. Two more open water assemblages with higher abundances of *Thalassiosira antarctica* T2 and *Chaetoceros* subg. *Hyalochaete*, are also identified. A longer spring season with open water is also associated with higher absolute diatom abundances, driven primarily by high abundances of the spring bloom group *Chaetoceros* subg. *Hyalochaete*. Pike et al. (2008) compared surface water and sea ice samples with modern core top data from the western side of the AP. Their data also highlight the role of sea surface temperature and timing of sea ice retreat in controlling diatom assemblages. More recently, Swilo et al. (2016) studied core top samples from coastal sites along the western AP. Their findings are similar to those of Buffen et al. (2007) and Pike et al. (2008), but present additional information on the distribution of benthic and epiphytic flora in shallow water sites, and the potential role of dissolution in concentrating more robust forms, such as *Fragilariopsis kerguelensis* and *Eucampia antarctica*.

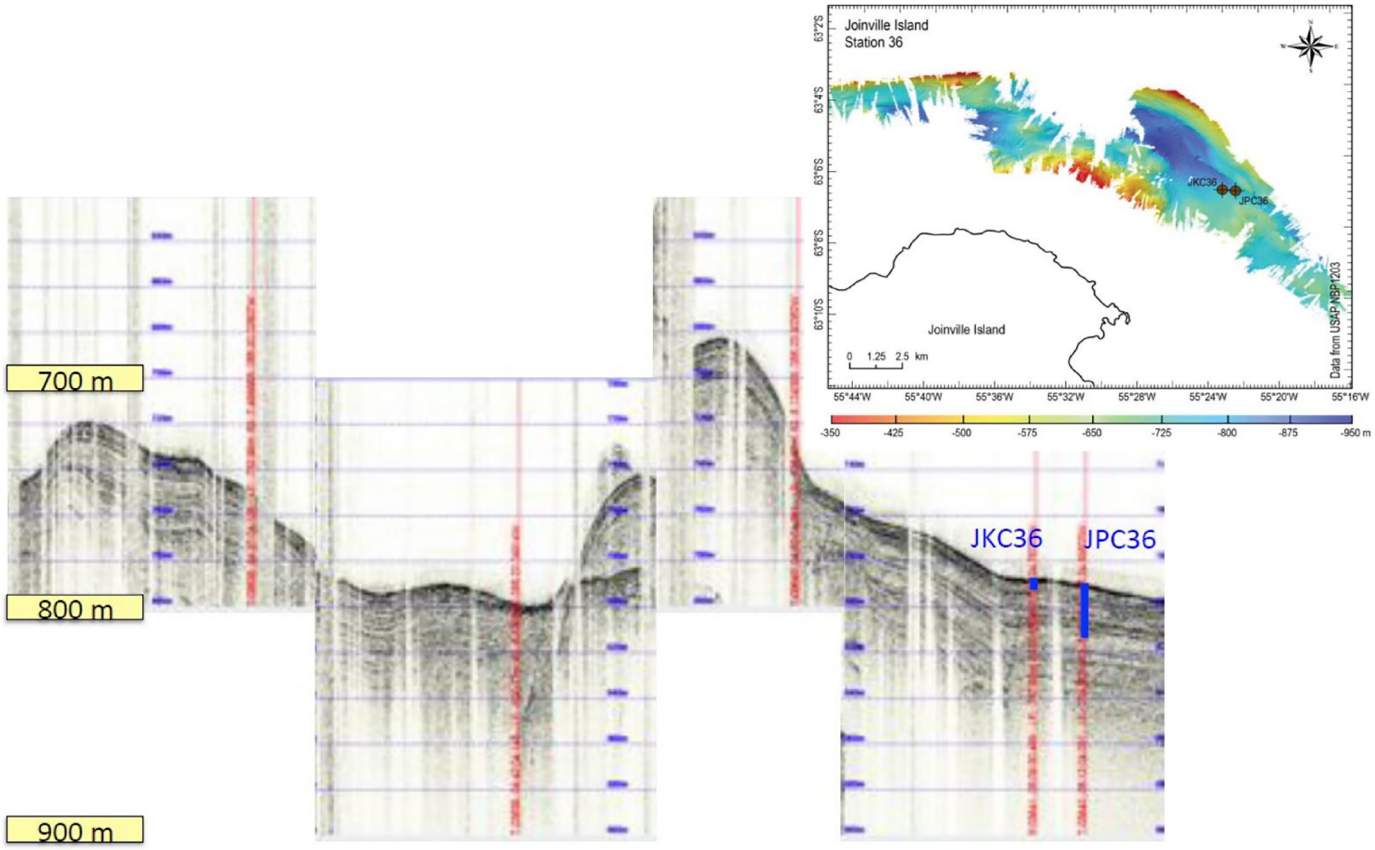

Fig. 2. Sub-bottom 3.5 kHz chirp profile through core sites JKC36 and JPC36. Inset image shows multibeam bathymetry with core locations.

3. Materials and methods

3.1. Field methods

Perseverance Drift was sampled in May 2012 during the *Nathaniel B. Palmer* cruise 2012–03 (NBP12–03) as part of the LARISSA (LARsen Ice Shelf System Antarctica) project. Core sites were selected using multibeam bathymetry and a Knudsen 3.5 kHz chirp profiler (Fig. 2), which revealed a complex subsurface containing at least 90 m of acoustically laminated sediment. Following the geophysical survey, two cores were collected from the PD: (1) jumbo kasten core 36 (JKC36; 63°05.35 S, 55°24.67 W, 806 m water depth), and (2) jumbo piston core 36 (JPC36; 63°05.34S, 55°23.92 W, 806 m water depth). The cores provide a complete recovery from 0 to 2382 cm.

3.2. Laboratory methods

3.2.1. Foraminifera

A total of 321 samples from cores JKC36 and JPC36 were analyzed for foraminifera. Sampling intervals in JKC36 ranged from 1 cm in the upper section (0–35 cm) of the core to 5 cm in the lower section (39–515 cm) of the core. JPC36 was sampled every 10 cm. The samples were washed through a 63 μm sieve and the ≥63 μm fraction was dried at ~50 °C and picked for foraminifera. A total of approximately 300 individuals were collected and counted from every sample where possible. The approximate sample volume is 10 cm^3 for the piston core (JPC36) and 20 cm^3 for the kasten core (JKC36). From this volume, the estimated number of foraminifera per cm^3 of wet sediment was determined (Appendix). For those samples yielding < 300 specimens, the entire sample volume was examined and picked for foraminifera. Therefore, the reported number of foraminifera per cm^3 is exact. For those samples yielding > 300 specimens, a fraction of the total sample was examined and picked (approximately 300–400 specimens). Therefore, the number of foraminifera per cm^3 is greater than that reported. Partial specimens were counted only when identifiable. Specimens were organized in micropaleontological slides and identified.

3.2.2. Diatoms

Sampling intervals in JKC36 ranged from 25 cm for the interval 0–450 cm to 5 cm or 10 cm in the lower section of the core (450–518 cm). JPC36 was sampled every 50 cm. For each sample, 20–25 mg of dry sediment was weighed, then processed with hydrogen peroxide at 50 °C to remove organic material. Quantitative diatom slides were produced according to the settling method described by Scherer (1994). This method involves settling a known amount of sediment over a known surface area, yielding a random distribution of diatoms for quantitative evaluation. Observations were made at 1000× magnification on an Olympus microscope (BX50, BX60, or CX31), and valves were identified to at least the genus level and species level where possible. For every 25 cm in JKC36, two sets of counting methods were applied due to the dominance of *Chaetoceros* subg. *Hyalochaete*. First, the total assemblage was counted in order to quantify the number of diatom valves per gram of sediment and percent of *Chaetoceros* subg. *Hyalochaete*. These data also allow calculation of the relative proportion of *Chaetoceros* resting spores versus vegetative valves. Second a *Chaetoceros*-free count was completed in order to assess the contribution of minor species to the total assemblage. For every 50 cm in JPC36, slides were counted for total assemblage and percent of *Chaetoceros* subg. *Hyalochaete*. At least 500 valves were counted along transects. Diatom abundances are presented in millions of valves per gram of dry sediment (mvpgs).

3.3. Multivariate statistical analysis of foraminiferal data

The foraminiferal data was analyzed with Q-mode principal component analysis (PCA) using PAST software (Hammer et al., 2001). PCA is a factor extraction technique in which samples are projected onto "best-fitting" principal component axes. The purpose of the analysis is to reduce the number of variables that were originally used to a smaller number of components by capturing as much of the variability in the original data set as possible (Abdi and Williams, 2010). In Q-mode PCA the scores represent the "alternate entities" and show the transformed value of the variables (foraminiferal species) contributing to each principal component. The loadings represent the relationship between the samples being loaded and the principal component axes and can be used to characterize the original species (Parker and Arnold, 2003; Abdi and Williams, 2010). When significant species have strong scores in one principal component, they are assumed to have overlapping environmental requirements and the principal component is referred to as the Foraminiferal Assemblage (FA) after the name of the species with the highest principal component score. PCA analysis in this study was performed on samples that included > 20 specimens, and species with relative abundances > 1% in at least one sample.

4. Chronology

A centimeter composite depth (cmcd) scale was constructed for cores JKC36 and JPC36 by correlating mass-normalized low-field magnetic susceptibility (χ_{LF}) profiles (Fig. 3). JKC36 contains unsupported ^{210}Pb in the uppermost 50 cm and is therefore assumed to have recovered an intact sediment-water interface. JKC36 was used as the reference core and its depths are unchanged. JPC36 was adjusted vertically downward to obtain the best match between meter-scale features in the two χ_{LF} profiles. No compression or expansion of the JPC36 depth scale was implemented. Sub-meter scale features could not be confidently correlated between the two cores due to the finely laminated nature of the sediment and suspected changes in unit thicknesses between the two core sites, which are separated by 600 m. The final cmcd scale applies a 180 cm downward adjustment to the JPC36 depths.

Mollusk fragments and articulated bivalves from JKC36 and JPC36 were used for radiocarbon dating. Samples were rinsed with deionized water, dried, and sent to the National Ocean Sciences Accelerator Mass Spectrometry (NOSAMS) Facility at Woods Hole Oceanographic Institute (WHOI), Woods Hole, MA. Radiocarbon ages were corrected with a regional reservoir age of 1260 ^{14}C years. This correction was chosen based upon published ^{14}C ages that were measured on modern and near-modern biogenic calcite in the AP region, which range from 1160 to 1300 ^{14}C yr BP (Berkman and Forman, 1996; Domack et al., 2001, 2005; Milliken et al., 2009). Radiocarbon ages were calibrated using CALIB version 7.1 and the MARINE13 dataset (Stuiver et al., 2017). Ages reported here are the CALIB median probabilities for each sample, which differ by only 2–20 years from the mid-point of the 2-sigma probability region. Uncertainties for the calibrated ages are reported as the half-width of the 2-sigma probability distribution region, rounded to the nearest 10 years (Table 1).

5. Results

5.1. Lithology

Cores JKC36 and JPC36 are composed of dark greenish-gray silty diatom mud and diatom ooze. The sediment texture alternates between thinly bedded to thinly laminated intervals interspersed with bioturbated intervals (Fig. 3).

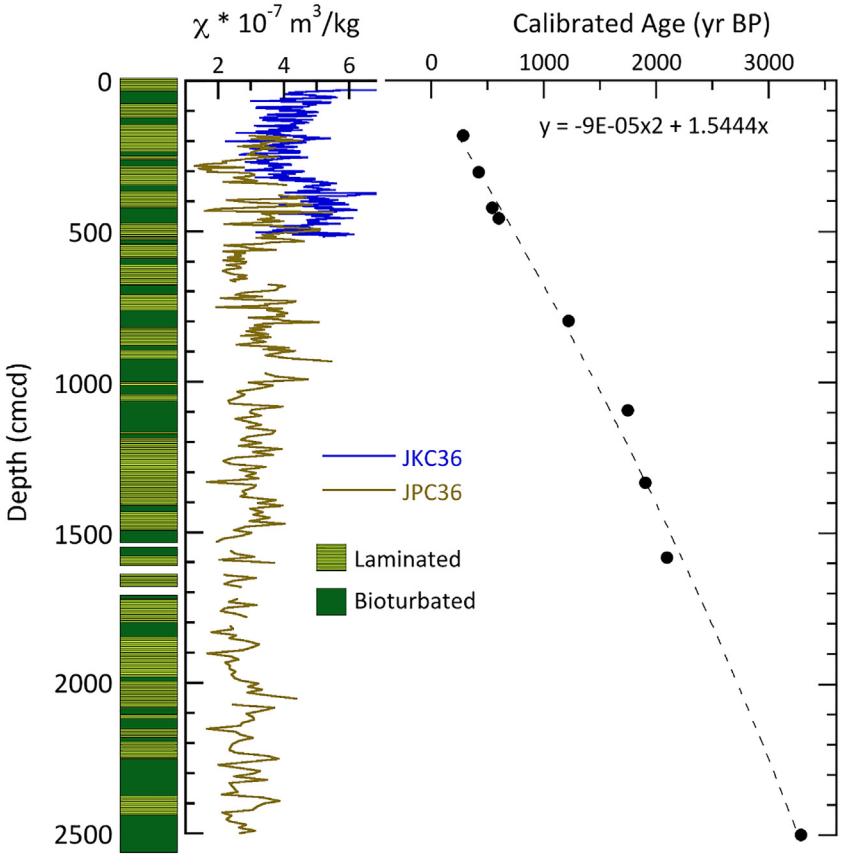

Fig. 3. (Left) Lithology and χ_{LF} for JKC36 (blue) and JPC36 (brown). (Right) Calibrated age vs. cmcd for the shell material from JKC36 and JPC36. The age vs. depth model is given by a 2nd order polynomial fit to the data in Table 1, with the curve constrained to intersect the origin. The depth-age equation is $y = -9E\text{-}5x^2 + 1.5444x$, where y = age in yr BP, x = depth in cmcd, and $R^2 = 0.99236$. (For interpretation of the references to color in this figure legend, the reader is referred to the web version of this article.)

Table 1
Radiocarbon samples.

NOSAMS #	Carbon source	Core	Depth (cmbsf)	[a]Depth (cmcd)	Raw age (^{14}C yr BP)	Error (yr)	[b]Corrected age (^{14}C yr BP)	Calibrated age (yr BP)	[c]Age error (yr)
122558	Shell fragment	JPC36	1	181	1500	20	240	284	10
122562	Shell fragment	JKC36	303.25	303.25	1630	20	370	422	70
122561	Shell fragment	JKC36	421	421	1810	20	550	543	50
122556	Bivalve	JPC36	275.5	455.5	1880	20	620	598	20
122554	Shell fragment	JPC36	616	796	2510	20	1250	1220	50
122560	Shell fragment	JPC36	912	1092	3010	20	1750	1744	80
122559	Shell fragment	JPC36	1151.5	1331.5	3150	20	2250	1900	70
122557	Bivalve	JPC36	1400	1580	3310	20	2050	2094	90
122555	Bivalve	JPC36	2319	2499	4270	20	3010	3284	70

[a] cm composite depth scale (cmcd) was calculated by adding 180 cm to the JPC36 cmbsf depths.
[b] A regional reservoir age of 1260 ^{14}C yr was used to correct the raw ages. This was implemented in CALIB7.1 by adding a ΔR value of 860 yr to the default reservoir age of 400 yr.
[c] Uncertainties for calibrated ages are the half-width of the 2-sigma probability region, rounded to the nearest 10 years.

5.2. Foraminiferal census data

A total of 16 foraminiferal taxa were identified between 0 and 2562 cmcd. The identification revealed 12 benthic arenaceous taxa, 3 benthic calcareous taxa and 1 planktonic taxon (*Neogloboquadrina pachyderma*, Ehrenberg) occurring in small numbers in the lower portion of the composite record. The foraminiferal abundances exhibit variable but rather low concentrations, while in only two intervals (179.5 and 265.5 cmcd) diversity exceeds 15 species per sample (Appendix). Some of the groupings include several species and are indicated as spp. *Globocassidulina* spp. include *Globocassidulina biora* (Crespin), *Globocassidulina subglobosa* (Brady) and *Globocassidulina* sp. *Nodulina* spp. include *Nodulina dentaliniformis* (Brady) and *Nodulina kerguelensis* (Parr). *Nonionella* spp. include *Nonionella iridea* (Heron-Allen and Earland) and *Nonionella bradii* (Chapman). *Labrospira* spp. include *Labrospira jeffreysii* (Williamson) and *Labrospira wiesneri* (Parr). *Miliammina* spp. include *Miliammina oblonga* (Heron-Allen and Earland) and *Miliammina lata* (Heron-Allen and Earland).

Relative abundances of selected (exhibiting higher relative abundances) foraminiferal species and taxa are presented in Fig. 4. *Miliammina* spp. are abundant throughout the entire record, though exhibiting variable concentrations (1–91%). Other important agglutinated species that are present regularly include *Paratrochammina lepida* (2–63%), *Paratrochammina bartami* (1.6–51%), and *Portatrochammina antarctica* (0–52%). Agglutinated species *Adercotryma glomerata* (0–11%) and *Rhumberella* sp. (0–32%) show their highest abundances between the 0 and ~500 cmcd, progressively decreasing downcore and becoming sparse after ~1000 cmcd. Calcareous *Globocassidulina* spp. (0–77.5%) and *Fursenkoina fusiformis* (0–36.8%) are highly abundant in thin intervals from the base of the record to ~1600 cmcd, followed by an interval where they are absent from the record, until reappearing in short, distinct intervals at the top of the composite record (approximately 150 to 350 cmcd).

5.3. Results from the foraminiferal PCA analysis

Results from PCA indicated 3 PC axes, denoted PCA1-PCA3, which explain 89.85% of the variance in the data. The five dominant foraminiferal taxa are represented by three foraminiferal assemblages (FA) that are named after the taxa with the highest PC scores. *Miliammina*

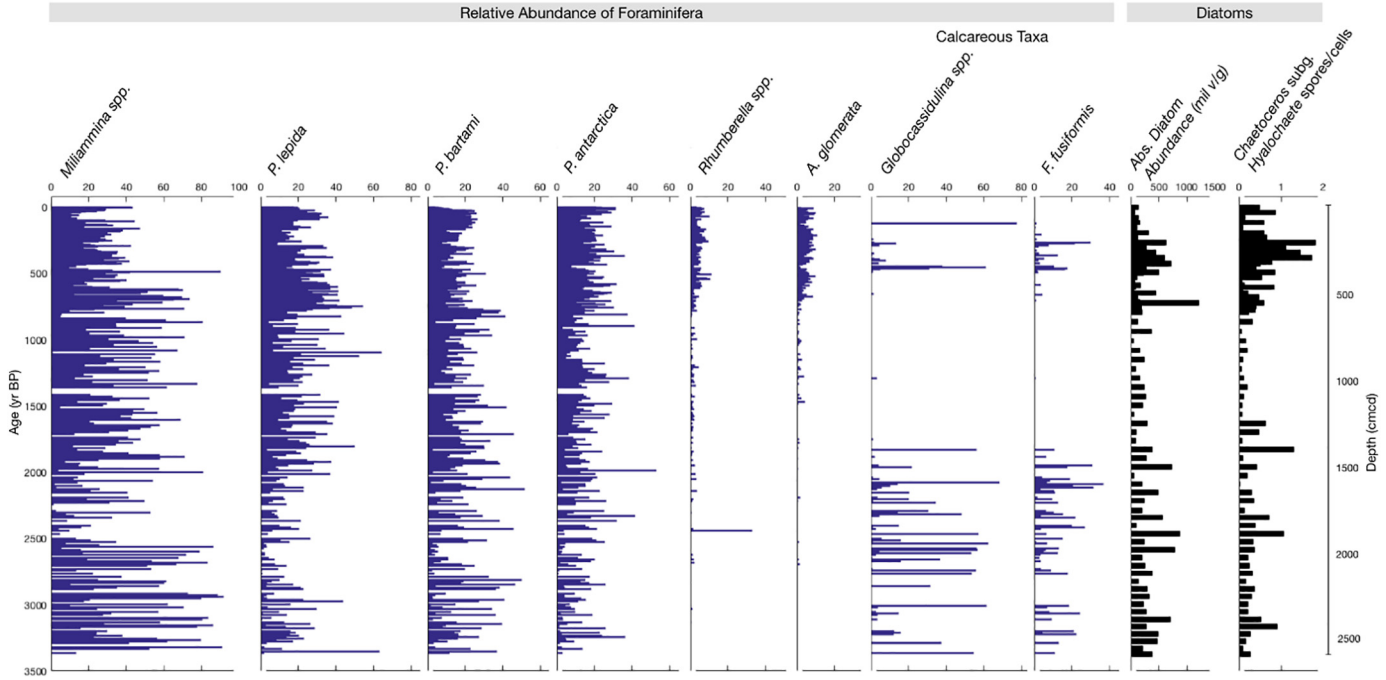

Fig. 4. Relative abundances of selected agglutinated and calcareous benthic foraminifera taxa, absolute diatom abundance (millions of valves/g dry sediment), and the ratio of *Chaetoceros* subg. *Hyalochaete* resting spores/vegetative cells data from the Perseverance Drift composite record.

Table 2
Foraminiferal PCA scores of the Perseverance Drift Composite record, showing scores of the foraminifera taxa that comprise the Faunal Assemblages (FAs).

Variable	PC1	PC2	PC3
%Explained variance	64.45	16.80	8.60
Benthic agglutinated taxa			
Portatrochammna antarctica	0.57	**1.20**	0.27
Paratrochammina lepida	0.50	**1.42**	0.37
Paratrochammina bartami	0.69	**2.53**	0.66
Miliammnina spp.	**3.09**	−1.51	−0.39
Rhumberella sp.	−0.40	−0.02	−0.50
Spiroplectammina biformis	−0.43	−0.18	−0.61
Textularia antarctica	−0.51	−0.28	−0.63
Textularia wiesneri	−0.53	−0.27	−0.61
Adecrortyma glomerata	−0.39	0.01	−0.49
Labrospira spp.	−0.49	−0.18	−0.54
Nodulina spp.	−0.55	0.31	0.60
Benthic calcareous taxa			
Globocassidulina spp.	−0.48	−1.18	**3.13**
Fursenkoina fusiformis	−0.49	−0.47	0.06
Nonionella spp.	−0.55	−0.46	−0.10

Scores of species significant for proposed assemblages are shown in bold.

spp. FA explained 64.45% of the total variance. The *P. lepida/P. bartami/P. antarctica* FA explained 16.80% of the total variance, and *Globocassidulina* spp. FA explained 8.60% of the total variance (Table 2, Fig. 5). The component axes scores that are > 0.4 illustrate the most significant assemblages and the most important faunal transitions and display two major paleoclimatic Units. Unit 1 is characterized by statistically significant scores in PCA 1 (between ~2500 and 1300 cmcd: ca. 3400–1800 yr BP) and statistically significant scores in PCA axis 3. However, in this interval, PCA 3 scores do not seem to be dominating beyond the statistically significant threshold of 0.4. Therefore, Unit 1 is primarily represented by the *Miliammina* spp. FA and the *Globocassidulina* spp. FA. Unit 2 (between ~1300 cmcd-core top: ca. 1800–0 yr BP) is characterized by the disappearance of the *Globocassidulina* spp. FA, the stronger representation of the *P. lepida/P. bartami/P. antarctica* FA, while the *Miliammina* spp. FA remains dominant.

5.4. Diatom census results

Diatoms are abundant throughout the composite record and are dominated by *Chaetoceros* subg. *Hyalochaete* vegetative cells and resting spores that together comprise > 90% of the total species assemblage. In JKC36, the remaining 2–10% of the total diatom assemblage mainly consists of the species *Thalassiosira antarctica* with species of the genera *Cocconeis* and *Fragilariopsis* making up the remaining fraction. When excluding *Chaetoceros* subg. *Hyalochaete* in counts, *Thalassiosira antarctica* comprises about 40% of the diatom assemblage. *Fragilariopsis* spp. in JKC 36 (*F. curta*, *F. cylindrus*, *F. sublinearis*, *F. vanheurckii*) account for approximately one quarter of the total diatom *Chaetoceros*-free assemblage with fluctuations up to 20% from the average. The remainder of the diatom assemblage is characterized by a significant contribution of benthic diatom species, including *Cocconeis* spp. and to a lesser extent *Gomphonema* spp., which together comprise 10–20% of the *Chaetoceros*-free assemblage (Fig. 6).

6. Discussion

The foraminiferal PCA assemblage units (FAs) and diatom flora described above reflect oceanographic and glaciological conditions (sea

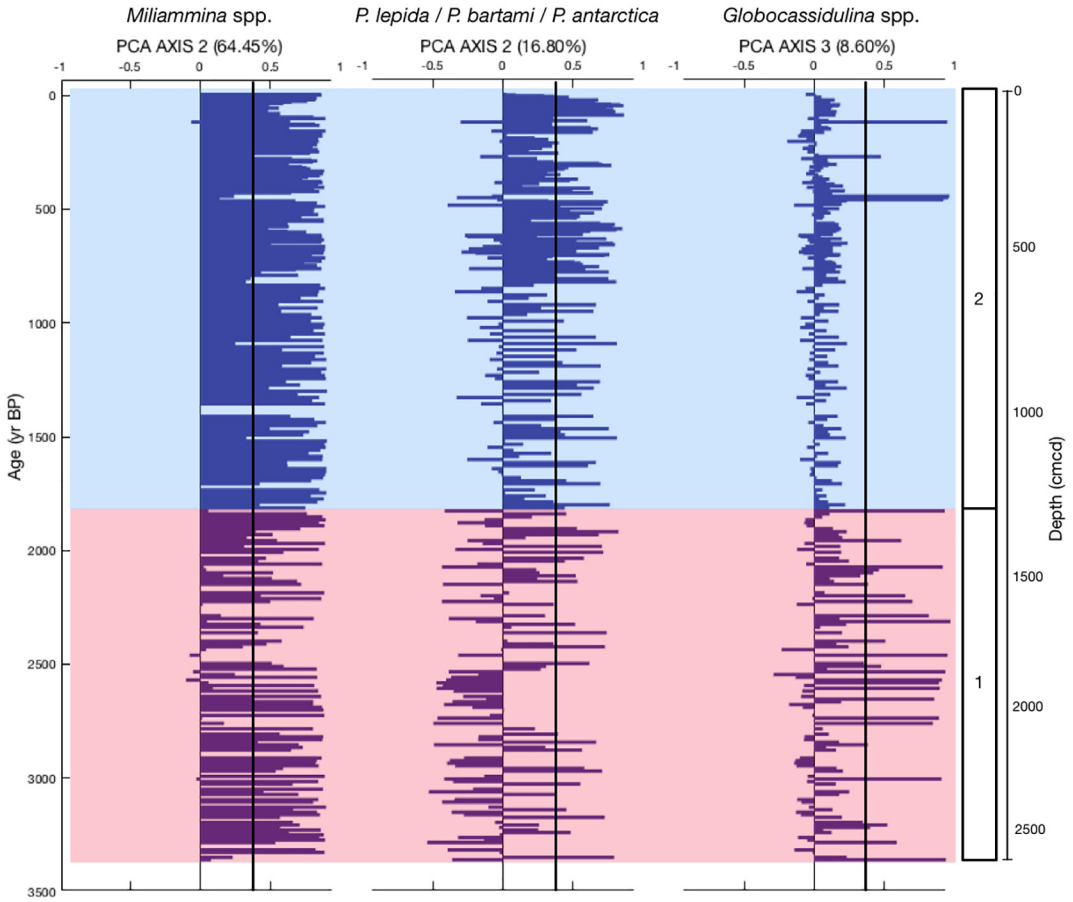

Fig. 5. Distribution of the major foraminiferal principal components for the composite record. PCA 1 represents *Milliammina* spp., PCA 2 represents *P. lepida/P. bartami/P. antarctica*. PCA 3 represents *Globocassidulina* spp. Statistically significant PCA loadings > 0.4 are delineated (Malmgren and Haq, 1982).

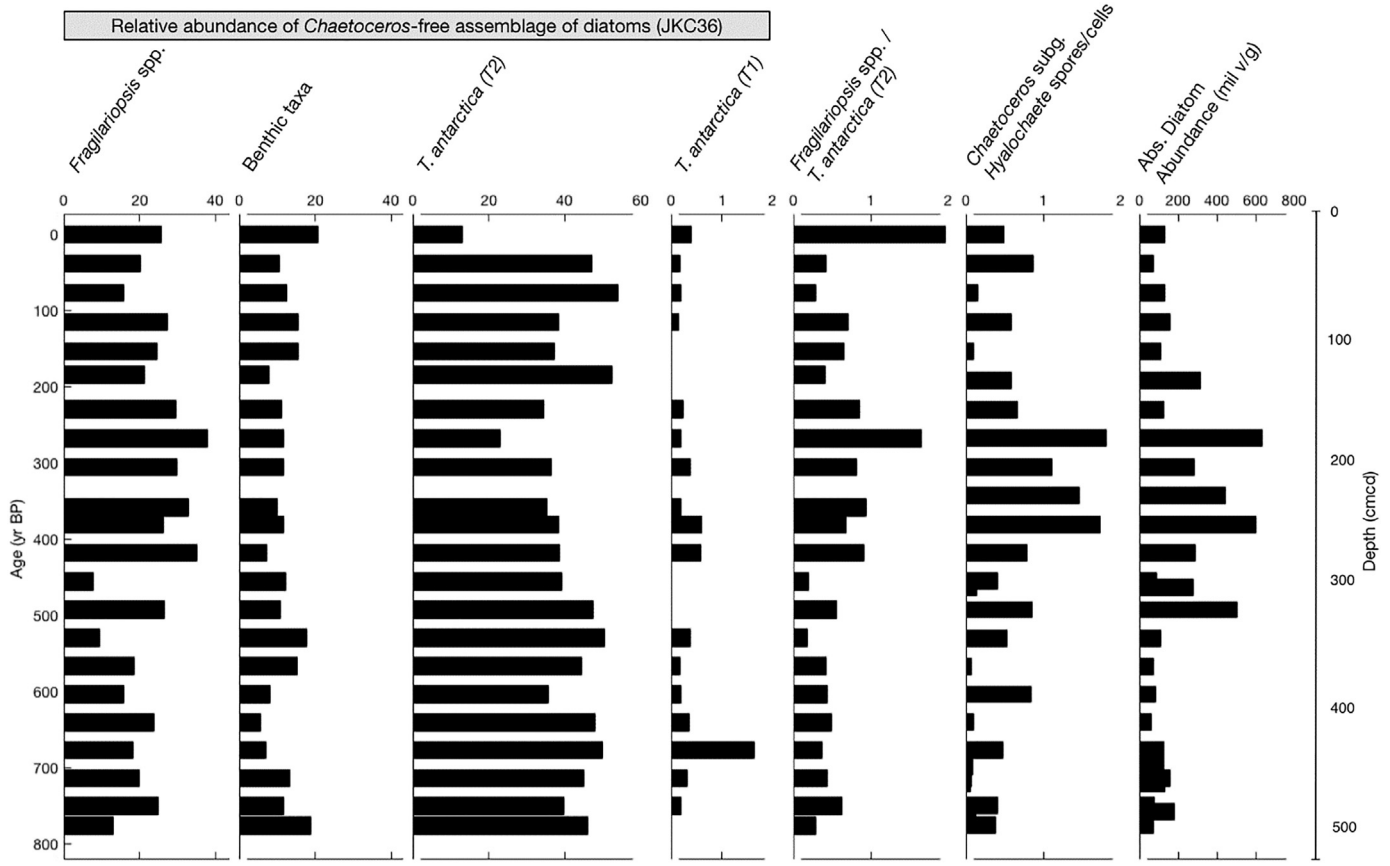

Fig. 6. Data from JKC36. Relative abundances of diatom species and groups of species (*Fragilariopsis* spp. include *F. curta*, *F. cylindrus*, *F. sublinearis*, *F. vanheurckii*; benthic diatom taxa include *Cocconeis* spp., *Gomphomena* spp., *Navicula* spp.) as based on quantitative counts within the *Chaetoceros*-free assemblage counts. Absolute diatom abundance (millions of valves/g dry sediment) and the ratio of *Chaetoceros* subg. *Hyalochaete* resting spores/vegetative cells are based on total counts.

ice cover, intensity of primary productivity, bottom current activity and bottom water mass circulation) during the late Holocene. Here we discuss the composition and environmental significance of the proposed FAs and diatom flora, primarily according to their environmental affinities, and also in the context of correlating them with regional climate records.

6.1. Foraminiferal assemblages

6.1.1. Miliammina spp. FA

The dominant taxa of PCA 1, *Miliammina* spp., are the most abundant group of foraminifera observed. Foraminiferal assemblages with high concentrations of *Miliammina* spp. are known from several circum-antarctic localities. A similar assemblage identified by Anderson (1975a) was interpreted as indicating the tolerance of the taxa to higher salinities when perennial ice and/or cold High Salinity Shelf Water - formed by the freezing process - characterized the shelf oceanographic conditions. *Miliammina*-rich foraminiferal assemblages off the Larsen A embayment (Ishman and Szymcek, 2003) and Gerlache Strait (Majewski et al., 2016) have been correlated with fine-grained, diatomaceous sediments with elevated organic content. The mid-Holocene benthic foraminiferal record from the Palmer Deep off the western Antarctic Peninsula coast was dominated by a *M. arenacea* assemblage, which Ishman and Sperling (2002) interpreted as indicative of the presence of cold, corrosive Saline Shelf Water circulating in the poorly ventilated Palmer Deep basin in the absence of Circumpolar Deep Water. At the Firth of Tay, a bay south of Joinville Island and in close proximity to Perseverance Drift, the *M. arenacea* FA became dominant in the mid-Holocene, between 7750 and 6000 yr BP, possibly corresponding to seasonally open marine conditions and higher primary productivity in the area (Majewski and Anderson, 2009).

In this study the *Miliammina* spp. assemblage is present throughout the entire record. The consistently high absolute diatom abundance, combined with the dominance of spring bloom diatom genus *Chaetoceros* subg. *Hyalochaete*, and relatively open water coastal species *T. antarctica*, suggest a productive open marine setting for the area. This could have led to increased corrosiveness of bottom water due to decomposition of organic matter, and the consequent preservation of dissolution resistant *Miliammina* spp. as compared to other, more easily dissolved species of foraminifera. The overall dominance of the *Miliammina* spp. assemblage suggests that the preservation potential of the species is high enough that they do not dissolve under the local carbonate saturation state and redox conditions (Schmiedl et al., 1997). However, since *Miliammina* spp. are present throughout the composite record, their presence does not signify any large-scale paleoceanographic changes in the area, except possibly fluctuations in the extent of sea ice.

6.1.2. Globocassidulina spp. FA

The *Globocassidulina* spp. FA is the dominant FA in PCA 3, in Unit 1, and characterizes the oldest section of the record. Although PCA analysis did not group *Globocassidulina* spp. with *Fursenkoina fusiformis* in an assemblage, the two taxa are associated since elevated percentages of *Globocassidulina* spp. are accompanied by *F. fusiformis* individuals (Fig. 4). In this context, the *Globocassidulina* spp. FA of this study can be compared with the *Fursenkoina* spp. FA from the Gerlache and Bransfield Straits in the Bellingshausen margin of the Antarctic Peninsula, where *G. biora* and *G. subglobosa* are included as important constituents of the *Fursenkoina* spp. FA (Ishman and Domack, 1994). In this region primary productivity is high, and cold WSTW that moves out of the

Weddell Sea and down the western margin of the Antarctic Peninsula is the dominant bottom-water mass. A similar assemblage composed of opportunistic species that responded to high phytodetrital deposits following intense spring diatom blooms and high terrigenous sedimentation rates was documented in the benthic foraminiferal record from the early Holocene of the Palmer Deep. This period, between 12.6 and 9.0 ka, was interpreted as representing near-ice-edge conditions after ice shelf retreat (Leventer et al., 2002; Ishman and Sperling, 2002). According to Szymcek et al. (2007), the early to mid-Holocene section of the Vega Drift on the northeastern AP is characterized by the presence of highly productive yet non-corrosive bottom waters similar to Ice Shelf Water, which is a lighter and colder version of Saline Shelf Water that results from its mixing with glacial meltwater (Foldvik et al., 1985; Szymcek et al., 2007). In the Firth of Tay, the *Globocassidulina* spp. - *F. fusiformis* assemblage is interpreted to be representative of the most glacier-proximal conditions that dominated during the early-Holocene glacial retreat of the site (Majewski and Anderson, 2009; Michalchuk et al., 2009). There, the presence of *Cribroelphidium webbi*, a unique glacier-proximal indicator (Majewski and Tatur, 2009) supports the interpretation of glacial sedimentation (Majewski and Anderson, 2009; Majewski et al., 2016).

WSTW is to be expected to influence the study area. This water mass, or water generated by glacial retreat, drives down the salinity and temperature and allows for the proliferation and preservation of calcareous assemblages such as the *Globocassidulina* spp. Therefore, it appears that the *Globocassidulina* spp. FA represents less extensive sea ice after spring diatom blooms and *Globocassidulina* spp. are acting as opportunistic species that are responding to the elevated influx of organic carbon in seafloor sediment derived from high primary productivity in the upper water column (Alve, 1995, 2003). High values of organic carbon could also be explained in part by the transport of epiphytic diatoms from the littoral zone by downslope processes or shorefast sea ice transport processes (discussed later). Furthermore, the absence of *Bulimina aculeata*, which is associated with the presence of warm Circumpolar Deep Water (CDW) in the Bellingshausen Sea, argues against the incursion of a warm, productive bottom-water mass. This supports the interpretation of WSTS or a water mass with similar characteristics (Ishman and Domack, 1994) influencing the calcareous fauna.

Calcareous *Globocassidulina* spp. and *F. fusiformis*, occur in short and distinct intervals in the upper 500 cmcd, and appear to be less vulnerable to corrosive bottom water conditions. Those intervals might be responding to the elevated delivery of phytodetritus from the upper water column, as shown by the total diatom abundance in approximately the same intervals (Fig. 4), or they could be associated with sedimentation and/or remobilization of current-transported sediments from shallower depths. Previous researchers have noted an association of *Globocassidulina biora* (a constituent of the *Globocassidulina* spp. of this study) with high bottom water activity and coarser grain size distributions (Milam and Anderson, 1981; Mackensen et al., 1990). However, sedimentological data do not support down-slope redeposition of sediment from near-shore settings for the increased presence of *Globocassidulina* spp. in the upper section of the core.

6.1.3. *P. lepida/P. bartami/P. antarctica FA*

The *P. lepida/P. bartami/P. antarctica* FA characterizes the younger section of the core (Unit 2). High scores of the FA are accompanied by other agglutinated species/taxa of the study; *A. glomerata*, *Rhumberella* sp., *S. biformis*, *T. wiesneri* are initially absent in Unit 2, while progressively becoming more abundant as the core becomes younger. This assemblage is similar to the southwestern shelf area of the Weddell Sea identified by Anderson (1975a), where Saline Shelf Water circulates and surface freezing is pronounced. Szymcek et al. (2007) also identify a similar assemblage in Holocene samples from the Vega Drift dominated by additional agglutinated species in addition to the common *M. arenacea*. This assemblage was dominated by *T. wiesneri*, S. *biformis* and included *Portatrochammina* spp. Moreover, Ishman and Szymcek (2003) recognized the Prince Gustav Channel/Outer Larsen A modern biofacies, which is dominated by *Miliammina* and *Portatrochammina* spp. The composition of this assemblage is modified by dissolution associated with the circulation of Ice Shelf Water and lack of surface carbonate production, as shown by the lack of planktonic foraminifera. In the Firth of Tay, the *P. bartami-P. antarctica* FA becomes prominent in the younger part of the core, and is interpreted to be representative of glacier-distal, yet still cooler Neoglacial conditions at the site (Majewski and Anderson, 2009; Michalchuk et al., 2009). Perseverance Drift Unit 2 is consistent with descriptions of foraminiferal assemblages that could result from freezing and Saline Shelf Water formation. Consequently, calcareous species are a minor component and agglutinated species dominate.

6.2. *Diatom analysis*

In the Southern Ocean, taxa of the genus *Chaetoceros* subg. *Hyalochaete* and more specifically high concentrations of *Chaetoceros* subg. *Hyalochaete* resting spores have been interpreted as being indicative of high primary production during a spring bloom (Buffen et al., 2007; Crosta et al., 1997; Leventer, 1991, 1992). Leventer (1991) reports that *Chaetoceros* subg. *Hyalochaete* resting spores dominate the spring diatom assemblage in sediment traps from the Gerlache Strait and suggest that the observed spore formation resulted from nutrient depletion. Leventer et al. (2002), working on Holocene sediments from the Palmer Deep, suggested that the ratio of *Chaetoceros* subg. *Hyalochaete* resting spores to vegetative cells could be used as a proxy for nutrient depletion, driven by a combination of large spring blooms and stabilization of the upper water column, perhaps due to the presence of low salinity meltwater and/or calm conditions. Similarly, Crosta et al. (1997) note that *Chaetoceros* subg. *Hyalochaete* resting spores represent a specialized life cycle stage formed as a survival mechanism during unfavorable growth conditions including nitrogen depletion, after high primary production, and reduction of light during the polar winter. In the PD cores, the dominance of *Chaetoceros* subg. *Hyalochaete* (> 90%) indicates the consistent occurrence of a large spring bloom. The increased ratio (≥1) of *Chaetoceros* subg. *Hyalochaete* resting spores to vegetative cells in the upper section of the composite core, between ~150 and 300 cmcd: ca 250–450 yr BP suggests that this time period may have been characterized by nutrient depletion.

The remaining 2–10% of the total diatom assemblage in JKC36 mainly consists of the species *Thalassiosira antarctica* T2, which comprises about 40% of the *Chaetoceros*-free diatom assemblage. *Thalassiosira antarctica* abundances have been reported from sediments of marginal ice edge environments around Antarctica (Leventer and Dunbar, 1987, 1988, 1996; Leventer, 1992; Zielinski and Gersonde, 1997). The valves observed in JKC36 are generally very large in diameter. Villareal and Fryxell (1983) cultured *T. antarctica* at two temperatures, 4.0 °C and 1.0 °C, and observed that at the higher temperature, *T. antarctica* grew to a larger size and possessed external tubes and coarser areolation. This allows for the identification of two distinct varieties of this species, a cold (T1) and warm (T2) morphotype (Taylor et al., 2001). In surface sediments from the eastern side of the Antarctic Peninsula, Buffen et al. (2007) observed an inverse distribution of the two forms of *T. antarctica*, with greater abundances of the "warm" morphotype in the open coastal Prince Gustav Channel and northeastern-most Peninsula and a decreasing southwestward trend of abundance towards the Larsen A embayment. These data support the distribution of the "warm" morphotype in coastal, less extensively ice-covered regimes.

Sea ice associated *Fragilariopsis*, including *F. curta, F. cylindrus, F. sublinearis,* and *F. vanheurckii* comprise about one quarter of the total diatom *Chaetoceros*-free assemblage with fluctuations up to 20% from the average. *F. curta* and *F. cylindrus* grow successfully in sea ice and sea ice edge ecosystems (Leventer, 1998). The ratio of *Fragilariopsis* spp. to

T. antarctica in JKC36 highlights the interval from ~150–300 cmcd (ca. 250–450 yr BP) as one characterized by increased relative abundance of *Fragilariopsis*, suggesting the dominance of sea ice associated primary productivity at that time, in contrast to a more open water environment. In combination with the *Chaetoceros* data, which suggest nutrient depletion at this time, it is likely that surface waters were well stratified, possibly due to the presence of greater sea ice melt.

Finally, benthic diatom species, including *Cocconeis* spp. and *Gomphonema* spp., comprise 10–20% of the *Chaetoceros*-free assemblage. *Cocconeis* spp. are commonly found as epiphytic organisms living attached to macro- and micro- algal species (Al-Handal et al., 2010 - Potter Cave, King George Island; Majewska et al., 2013 - Terra Nova Bay, Ross Sea). The observation of relatively high abundances of epiphytic diatoms suggests that the valves observed in JKC36 originated in the shallow, well-lit littoral zone attached to macroalgae, and their transport to deeper water was facilitated through downslope processes and/or transport by shorefast sea ice. Yoon et al. (2010) observe macroalgae entrained into coastal, shorefast sea ice on Maxwell Bay, King George Island, northwest of the Perseverance Drift site, and suggest they contribute as a potential organic carbon source. However, the absence of sedimentological data suggesting downslope remobilization and deposition of sediments leads us to suggest offshore rafting and deposition of the epiphytic diatoms in the Perseverance Drift site.

6.3. Paleoclimatic units

The Perseverance Drift record presented here spans a time period of ca. 3400 yr. For the duration of the record, the study area is characterized as a productive open-marine setting, but at times the climate was cooler with variations in sea ice extent. In general, the consistent presence of *Miliammina* spp., high absolute diatom abundances, and the dominance of the spring-blooming diatom *Chaetoceros* subg. *Hyalochaete* throughout the record indicate high primary productivity in the area. Given that vegetative valves generally dominate over resting spores, it is likely that nutrient limitation is infrequent (Fig. 4).

6.3.1. Unit 2: ~2500–1300 cmcd (ca. 3400–1800 yr BP)

The benthic foraminiferal record delineates two major oceanographic/climatic intervals of the middle and late Holocene. The older portion of the core from the base of ~2500 cmcd to ~1300 cmcd, corresponding to ca. 3400 yr BP to 1800 yr BP, is characterized by high abundances of *Globocassidulina* spp., which together with the presence of *F. fusiformis*, could be indicative of high primary productivity dominated by the influence of WSTW.

A mid-to-late Holocene climatic optimum has been described in several paleoenvironmental records around the AP region (Ingólfsson et al., 2003; Bentley et al., 2009), though the timing of the warm period varies among the records. This period lasted approximately 2000 years, roughly between 4.5 and 2.5 ka BP (Hjort et al., 2003; Ingólfsson et al., Bentley et al., 2009), after which the Neoglacial shift to colder climatic conditions occurred (Fig. 7). The marine record from Lallemand Fjord, western AP, documents the climatic optimum in sediments older than 2500 yr BP, manifested as increased % TOC values (Shevenell et al., 1996). The Middle Holocene of the Palmer Deep record (9–3.7 ka) indicates a period when the circulation of Saline Shelf Water and the seasonal stratification of surface water masses were promoting high primary productivity at the site (Leventer et al., 2002; Ishman and Sperling, 2002). The collapse of Prince Gustav Ice Shelf in the northwestern Peninsula has also been associated with Mid-Holocene warmth. After the transition from grounded to floating ice in Prince Gustav Channel at 11 ka (Pudsey and Evans, 2001), the ice shelf persisted until its retreat at 5 ka, when this area was exposed to seasonally open water intervals and reduced sea ice coverage (Pudsey et al., 2006). Björck et al. (1996) report a Holocene climatic optimum at 3 to 4.3 ka in lake sediments on James Ross Island. Sedimentary records from beneath the former Larsen A Ice Shelf indicate ice shelf stability during the early Holocene, followed by a transition to less stable conditions and episodes of ice shelf decay, manifested as a series of diatomaceous ooze layers and the appearance of calcareous planktonic foraminifera (Brachfeld et al., 2003). The lowest stratigraphic Unit in the Larsen A record contains gravelly mud and transitions to more diatomaceous sediments by ca. 6.3 ± 0.5 ka, a time that broadly coincides with the onset of Hypsithermal conditions observed in records from the western and eastern sides of the Peninsula. Moreover, the Holocene diatomaceous layers dated 1.4 ± 0.25 ka, 2.1 ± 0.25 ka and 3.8 ± 0.5 ka suggest a prolonged period of warmer conditions (Brachfeld et al., 2003).

The PD record suggests that the middle-to-late Holocene climatic optimum was broadly contemporaneous along the AP with discrepancies reflected in both the onset and duration of the ameliorated conditions. Between ca. 3400 and 1800 yr BP the PD experienced periods of open marine conditions associated with the intrusion of WSTW. However, during this period the PD record appears to lag behind Palmer Deep and Firth of Tay records and be more in phase with the Lallemand Fjord and Prince Gustav Channel records.

6.3.2. Unit 1: ~1300 cmcd-surface (ca. 1800 cal yr-present)

The interval 0 to 1300 cmcd corresponds to ca. 1800 yr BP to the present. Higher eigenvalues of *P. lepida-P. bartami* and *P. antarctica* FA, along with other agglutinated taxa (*A. glomerata, Rhumberella* sp.) characterize this interval, and coincide with the absence of calcareous taxa. Increased glaciation and/or increased sea ice formation would have led to the production of Saline Shelf Water, which inhibits calcareous foraminiferal presence and preservation. However, agglutinated species thrive in these conditions (Anderson, 1975a). Accordingly, this Unit could represent colder Neoglacial conditions at the Perseverance Drift site.

The Neoglacial, an interval of colder climate and more persistent sea ice, is observed in several AP records, though with asynchronous timing (Bentley et al., 2009). On the eastern AP, the onset of the Neoglacial is recorded in the Larsen A embayment and Prince Gustav Channel at 1.4 ka and 1.9 ka respectively (Brachfeld et al., 2003; Pudsey et al., 2006), which agrees well with the 1.8 ka onset observed in this study. However, the Firth of Tay record documents an earlier onset of the Neoglacial at 3.5 ka BP (Majewski and Anderson, 2009; Michalchuk et al., 2009). Similarly, the James Ross Island ice core record documents atmospheric cooling starting at 2500 yr BP, with pronounced cooling (0.7 ± 0.3 °C cooler than present) between 800 and 400 yr BP (Mulvaney et al., 2012). Lacustrine records from James Ross Island document cold and arid conditions from ca. 3 ka BP until ca. 1.2 ka yr, indicated by the disappearance of the glaciers in the area and the transformation of large lakes into enclosed, brackish water bodies (Björck et al., 1996). In the marine record from Lallemand Fjord, western AP, % TOC values decrease and the fjord displays ice shelf influenced characteristics, reflecting the formation and fluctuation of Muller Ice Shelf, at about 2.7 ka BP (Shevenell et al., 1996; Domack et al., 2003). Domack et al. (2001) recognized the onset of the Neoglacial interval in the marine record from the Palmer Deep starting at 3 ka BP.

The onset of Neoglacial conditions at ca. 1800 yr BP at the PD is broadly consistent with other sites across the AP. The absence of calcareous foraminifera and the appearance of sea ice-related species suggest that persistent sea ice was established in the study area associated with the circulation of Saline Shelf Water. However, the transition from Hypsithermal to Neoglacial conditions in the PD record appears to be delayed with respect to the Palmer Deep and Firth of Tay records and correlate better with the Lallemand Fjord and PGC records.

7. Conclusions

We present a paleoceangraphic and paleoenvironmental history for the northeastern AP for the past 3400 yr. The interval 3400–1800 yr BP is characterized by high primary productivity, shown by the abundance

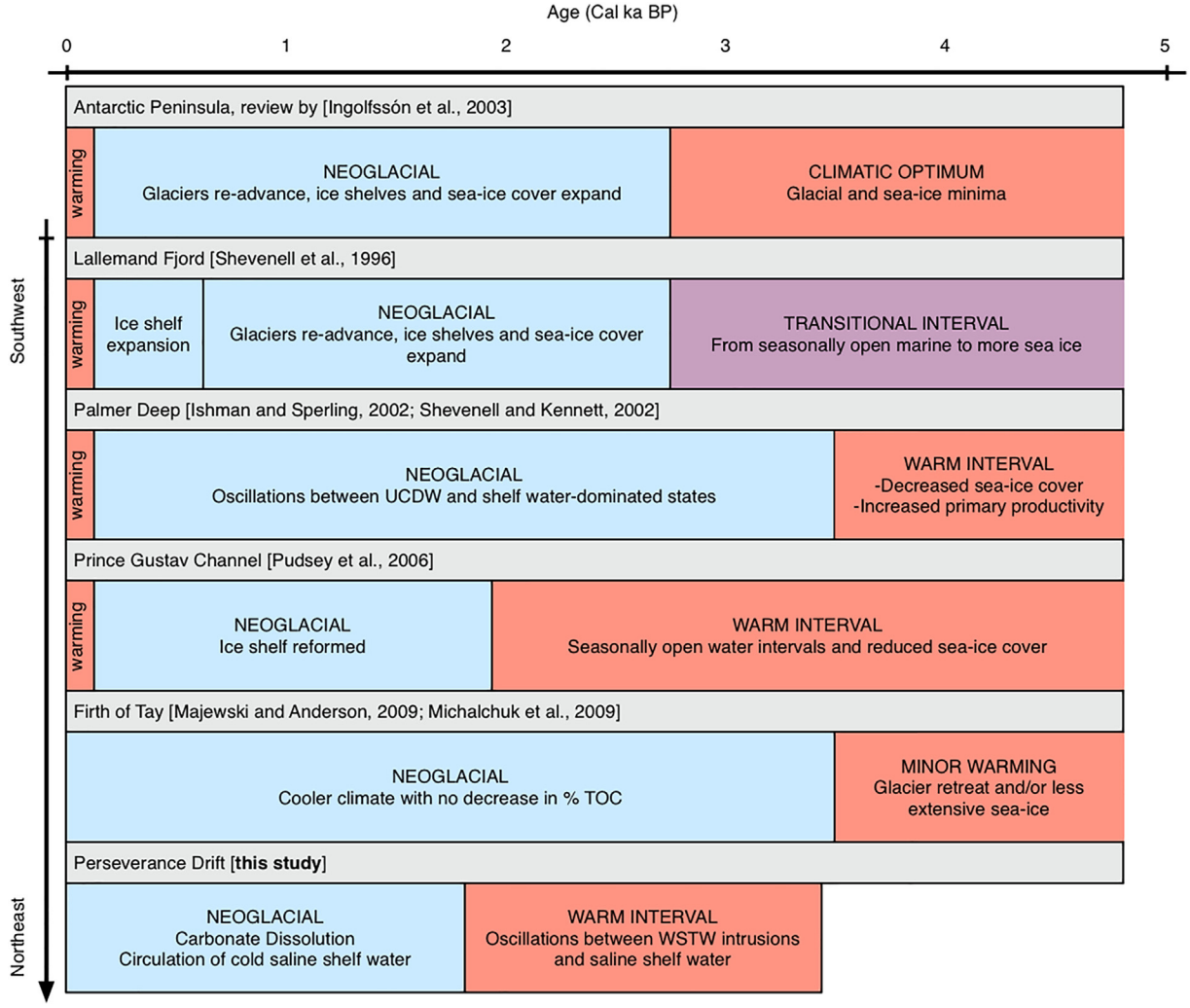

Fig. 7. Multi-archive compilation of middle-to-late Holocene phasing in the Antarctic Peninsula based on reconstructions from marine sediment records organized geographically from southwest to northeast and compared with this study (modified from Allen et al., 2010). Red bands show periods where relatively warm intervals have been interpreted. Blue bands show where Neoglacial conditions have been interpreted. Purple band indicates the end of Hypsithermal conditions in Lallemand Fjord and the transition to Neoglacial conditions. (For interpretation of the references to colour in this figure legend, the reader is referred to the web version of this article.)

of calcareous *Globocassidulina* spp., which together with the presence of *F. fusiformis* and high absolute diatom abundance is indicative of an open marine regime. It appears that WSTW allows for the preservation and proliferation of the calcareous foraminiferal fauna. More specifically, the *Globocassidulina* spp. are acting as opportunistic species corresponding to the elevated influx of organic content in seafloor sediments. We interpret this to represent warmer climatic conditions that persisted in the eastern AP during the mid-Holocene Hypsithermal. The interval 1800 yr BP to present records slightly colder conditions, manifested by the absence of calcareous *Globocassidulina* spp. and the pronounced presence of agglutinated *P. bartami-P. lepida* and *P. antarctica* FA, along with other agglutinated species that are indicative of the presence of heavier sea ice. Increased glaciation and/or increased sea ice formation could have led to the production of Saline Shelf Water, which inhibits the calcareous foraminiferal fauna from being present and preserved. This Unit corresponds to the onset of the Neoglacial Interval.

The high absolute diatom abundance and dominant assemblage of *Chaetoceros* subg. *Hyalochaete* (> 90%) throughout the composite core indicates high primary productivity in the region. Nutrient depletion, as indicated by higher ratios (≥1) of *Chaetoceros* resting spores to vegetative cells, occurs only between ~150 and 300 cmcd (ca. 250–450 yr BP). The nearshore environment and shallow shelf setting surrounding the Perseverance Drift, between Joinville and D' Urville Islands, plays a role in supplying nutrients and organic material to deeper waters. Abundant *Cocconeis* spp. in JKC36 are interpreted as benthic epiphytes and suggest transport of algal detritus to deeper water and the seafloor.

The Perseverance Drift record provides insight into AP climatic trends during the middle-to-late Holocene. This site is an exceptional target for future coring of a high-resolution Holocene sedimentary record. The unusually high preservation of both shell material and calcareous foraminiferal taxa could be pivotal in the development of a well-dated Holocene paleoceanographic record for the northwestern Weddell Sea.

Acknowledgements

This work was supported by National Science Foundation grants 0732605, 0732625 and 0732554. We thank the captain, crew and scientific party of the RVIB *Nathaniel B. Palmer* for their efforts during cruise NBP12-03.

Appendix A. Benthic foraminiferal taxonomic list

All the foraminifera taxa identified in this study are alphabetically listed below. The plate and figure references are to the papers used for taxonomic identification.

Adercotryma glomerata (Brady). Jones (1994), plate 34, figs. 15–18.
Cibicides sp.

Fursenkoina fusiformis (Williamson). Ishman and Domack (1994), plate 2, fig. 7.

Globocassidulina spp. are used as *G. biora* (Crespin). Majewski and Anderson (2009), plate 4, fig. 10, *G. subglobosa* (Brady). Murray and Pudsey (2004), plate 2, figs. 12-13 and *Globocassidulina* sp.

Labrospira spp. are used as *Labrospira jeffreysii* (Williamson). Igarashi et al. (2001), plate 3, fig. 4a-b and *Labrospira wiesneri* Parr. Igarashi et al. (2001), plate3, fig. 5a-b.

Miliammina spp. are used as *Miliammina lata* Heron-Allen and Earland. Igarashi et al. (2001), plate 2, fig. 10a-b) and *Miliammina oblonga* Heron-Allen and Earland. Igarashi et al. (2001), plate 2, fig. 11a-b.

Nodulina spp. are used as *Nodulina dentaliniformis* (Brady). Igarashi et al. (2001), plate 2, fig. 13 and *Nodulina kerguelensis* (Parr). Igarashi et al. (2001), plate 2, fig. 14.

Nonionella spp. are used as *Nonionella bradii* (Chapman). Mackensen et al. (1990), plate 1, fig. 4 and *Nonionella iridea* Heron-Allen and Earland. Mackensen et al. (1990), plate 1, figs. 4-9.

Paratrochammina (Lepidoparatrochammina) bartami (Hedley, Hurdle and Budrett). Brönnimann and Whittaker (1988), figs. 22A-C, 23B-L, 24E.

Paratrochammina (Lepidoparatrochammina) lepida (Brönnimann and Whittaker). Brönnimann and Whittaker (1988), fig. 21A-L.

Portatrochammina antarctica antarctica (Parr). Brönnimann and Whittaker (1988), figs. 25D, 26H-K, 27D-I.

Rhumberella sp.

Spiroplectammina biformis (Parker and Jones). Ishman and Domack (1994), plate 1, fig. 4.

Textularia antarctica (Weisner). Ishman and Domack (1994), plate 1, fig. 2.

Textularia wiesneri (Earland). Ishman and Domack (1994), plate 1, fig. 3.

Appendix B. Supplementary data

Supplementary data to this article can be found online at https://doi.org/10.1016/j.marmicro.2018.03.001.

References

Abdi, H., Williams, L.J., 2010. Principal component analysis. Wiley Interdiscip. Rev. Comput. Stat. 2 (4), 433–459.

Al-Handal, A.Y., Riaux-Gobin, C., Wulff, A., 2010. *Cocconeis pottercovei* sp. nov. and *Cocconeis pinnata* var. *matsii* var. nov., Two new marine diatom taxa from King George Island, Antarctica. Diatom Res. 25 (1), 1–11.

Allen, C.S., Oakes-Fretwell, L., Anderson, J.B., Hodgson, D.A., 2010. A record of Holocene glacial and oceanographic variability in Neny Fjord, Antarctic Peninsula. The Holocene 20 (4), 551–564.

Alve, E., 1995. Benthic foraminiferal distribution and recolonization of formerly anoxic environments in Drammensfjord, southern Norway. Mar. Micropaleontol. 25 (2), 169–186.

Alve, E., 2003. A common opportunistic foraminiferal species as an indicator of rapidly changing conditions in a range of environemnets. Estuar. Coast. Shelf Sci. 57 (3), 501–504.

Anderson, J.B., 1972. Nearshore glacial-marine deposition from modern sediments of the Weddell Sea. Nature 240 (104), 189–192.

Anderson, J., 1975a. Ecology and distribution of foraminifera in the Weddell Sea of Antarctica. Micropaleontology 69–96.

Anderson, J.B., 1975b. Factors controlling $CaCO_3$ dissolution in the Weddell Sea from foraminiferal distribution patterns. Mar. Geol. 19 (5), 315–332.

Armand, L.K., Crosta, X., Romero, O., Pichon, J., 2005. The biogeography of major diatom taxa in Southern Ocean sediments: 1. Sea ice related species. Palaeogeogr. Palaeoclimatol. Palaeoecol. 223 (1), 93–126.

Armand, L., Ferry, A., Leventer, A., 2017. Advances in palaeo sea-ice estimation. In: Thomas, D. (Ed.), Sea Ice, 3rd ed. Wiley-Blackwell, Oxford.

Bentley, M.J., Hodgson, D.A., Smith, J.A., Cofaigh, C.Ó., Domack, E.W., Larter, R.D., Roberts, S.J., Brachfeld, S., Leventer, A., Hjort, C., Hillenbrand, C.-D., Evans, J., 2009. Mechanisms of Holocene palaeoenvironmental change in the Antarctic Peninsula region. The Holocene 19 (1), 51–69.

Berkman, P.A., Forman, S.L., 1996. Pre-bomb radiocarbon and the reservoir correction for calcareous marine species in the Southern Ocean. Geophys. Res. Lett. 23 (4), 363–366.

Björck, S., Olsson, S., Ellis-Evans, C., Håkansson, H., Humlum, O., de Lirio, J.M., 1996. Late Holocene palaeoclimatic records from lake sediments on James Ross Island, Antarctica. Palaeogeogr. Palaeoclimatol. Palaeoecol. 121 (3), 195–220.

Brachfeld, S., Domack, E., Kissel, C., Laj, C., Leventer, A., Ishman, S., Gilbert, R., Camerlenghi, A., Eglinton, L.B., 2003. Holocene history of the Larsen-a ice shelf constrained by geomagnetic paleointensity dating. Geology 31 (9), 749–752.

Brönnimann, P., Whittaker, J.E., 1988. The Trochamminacea of the Discovery Reports, a Review of the Trochamminacea (Protozoa: Foraminiferida) Described from South Atlantic and Antarctic Waters by Herron Allen and Earland (1932) and Earland (1933; 1934; 1936). British Museum of Natural History, London, pp. 1–152.

Buffen, A., Leventer, A., Rubin, A., Hutchins, T., 2007. Diatom assemblages in surface sediments of the northwestern Weddell Sea, Antarctic Peninsula. Mar. Micropaleontol. 62 (1), 7–30.

Cape, M.P., Vernet, M., Skvarca, P., Marinsek, S., Scambos, T., Domack, E., 2015. Foehn winds link climate-driven warming to ice shelf evolution in Antarctica. J. Geophys. Res. Atmos. 120. http://dx.doi.org/10.1002/2015JD023465.

Carmack, E.C., 1974. A quantitative characterization of water masses in the Weddell Sea during summer. In: Proceedings Deep-Sea Research and Oceanographic Abstracts. 21. Elsevier, pp. 431–443.

Cook, A.J., Vaughan, D.G., 2010. Overview of areal changes of the ice shelves on the Antarctic Peninsula over the past 50 years. Cryosphere 4 (1), 77–98.

Cook, A.J., Fox, A.J., Vaughan, D.G., Ferrigno, J.G., 2005. Retreating glacier fronts on the Antarctic Peninsula over the past half-century. Science 308 (5721), 541–544.

Crosta, X., Pichon, J.-J., Labracherie, M., 1997. Distribution of *Chaetoceros* resting spores in modern peri-Antarctic sediments. Mar. Micropaleontol. 29 (3), 283–299.

De Lavergne, C., Palter, J.B., Galbraith, E.D., Bernardello, R., Marinov, I., 2014. Cessation of deep convection in the open Southern Ocean under anthropogenic climate change. Nat. Clim. Chang. 4 (4), 278–282. http://dx.doi.org/10.1038/nclimate2132.

Domack, E.W., Leventer, A., Dunbar, R., Taylor, F., Brachfeld, S., Sjunneskog, C., Leg 178 Scientific Party, O.D.P., 2001. Chronology of the Palmer Deep site, Antarctic Peninsula: a Holocene paleoenvironmental reference for the circum-Antarctic. The Holocene 11, 1–9.

Domack, E.W., Burnett, A., Leventer, A., 2003. Environmental setting of the antarctic Peninsula. In: Antarctic Peninsula Climate Variability: Historical and Paleoenvironmental Perspectives. American Geophysical Union, pp. 1–13.

Domack, E., Duran, D., Leventer, A., Ishman, S., Doane, S., McCallum, S., Amblas, D., Ring, J., Gilbert, R., Prentice, M., 2005. Stability of the Larsen B ice shelf on the Antarctic Peninsula during the Holocene epoch. Nature 436 (7051), 681–685.

Fahrbach, E., Rohardt, G., Scheele, N., Schröder, M., Strass, V., Wisotzki, A., 1995. Formation and discharge of deep and bottom water in the northwestern Weddell Sea. J. Mar. Res. 53 (4), 515–538.

Fahrbach, E., Harms, S., Rohardt, G., Schröder, M., Woodgate, R.A., 2001. Flow of bottom water in the northwestern Weddell Sea. J. Geophys. Res. Oceans 106 (C2), 2761–2778.

Foldvik, A., Gammelsrød, T., Tørresen, T., 1985. In: Jacobs, S.S. (Ed.), Circulation and Water Masses on the Southern Weddell Sea Shelf: Oceanology of the Antarctic Continental Shelf. American Geophysical Union, Washinghton, D.C. p, pp. 5–20.

Foster, T.D., Carmack, E.C., 1976. Frontal zone mixing and Antarctic Bottom Water formation in the southern Weddell Sea. Deep Sea Res. Oceanogr. Abstr. 23, 301–317.

Gill, A., 1973. Circulation and bottom water production in the Weddell Sea. Deep-Sea Res. Oceanogr. Abstr. 20, 111–140.

Gille, S.T., 2002. Warming of the Southern Ocean since the 1950s. Science 295 (5558), 1275–1277.

Gooday, A.J., Rothe, N., Bowser, S.S., Pawlowski, J., 2003. Benthic Foraminifera: Encyclopedia of Ocean Sciences. Elsevier, Amsterdam, pp. 274–286.

Hammer, Ø., Harper, D., Ryan, P., 2001. PAST: paleontological statistics software package for education and data analysis. Palaeontol. Electron. 4, 1–9.

Hellmer, H.H., Huhn, O., Gomis, D., Timmermann, R., 2011. On the freshening of the northwestern Weddell Sea continental shelf. Ocean Sci. 7 (3), 305–316.

Hjort, C., Ingólfsson, Ó., Bentley, M.J., Björck, S., 2003. The late pleistocene and holocene glacial and climate history of the Antarctic Peninsula region as documented by the land and lake sediment records-a review. In: Antarctic Peninsula Climate Variability: Historical and Paleoenvironmental Perspectives, pp. 95–102.

Igarashi, A., Numanami, H., Tsuchiya, Y., Fukuchi, M., 2001. Bathymetric distribution of fossil foraminifera within marine sediment cores from the eastern part of Lützow-Holm Bay, East Antarctica, and its paleoceanographic implications. Mar. Micropaleontol. 42 (3), 125–162.

Ingólfsson, Ó., Hjort, C., Humlum, O., 2003. Glacial and climate history of the Antarctic Peninsula since the last glacial maximum. Arct. Antarct. Alp. Res. 35 (2), 175–186.

Ishman, S.E., Domack, E.W., 1994. Oceanographic controls on benthic foraminifers from the Bellingshausen margin of the Antarctic Peninsula. Mar. Micropaleontol. 24 (2), 119–155.

Ishman, S., Sperling, M., 2002. Benthic foraminiferal record of Holocene deep-water evolution in the Palmer Deep, western Antarctic Peninsula. Geology 30 (5), 435–438.

Ishman, S.E., Szymcek, P., 2003. Foraminiferal Distributions in the Former Larsen-A Ice Shelf and Prince Gustav Channel Region, Eastern Antarctic Peninsula Margin: A Baseline for Holocene Paleoenvironmental Change: Antarctic Peninsula Climate Variability: Historical and Paleoenvironmental Perspectives. pp. 239–260.

Jones, R.W., 1994. The Challenger Foraminifera. Oxford University Press, Oxford, pp. 1–149.
Jorissen, F.J., Fontanier, C., Thomas, E., 2007. Paleoceanographical proxies based on deep-sea benthic foraminiferal assemblage characteristics. Dev. Mar. Geol. 1, 263–325.
Lavoie, C., Domack, E.W., Pettit, E.C., Scambos, T.A., Larter, R.D., Schenke, H.-W., Yoo, K.C., Gutt, J., Wellner, J., Canals, M., Anderson, J.B., Amblas, D., 2015. Configuration of the Northern Antarctic Peninsula Ice Sheet at LGM based on a new synthesis of seabed imagery. Cryosphere 9, 613–629.
Leventer, A., 1991. Sediment trap diatom assemblages from the northern Antarctic Peninsula region. Deep Sea Res. Part A 38 (8), 1127–1143.
Leventer, A., 1992. Modern distribution of diatoms in sediments from the George V Coast, Antarctica. Mar. Micropaleontol. 19 (4), 315–332.
Leventer, A., 1998. The fate of Antarctic “sea ice diatoms” and their use as paleoenvironmental indicators: Antarctic sea ice: biological processes, interactions and variability. Antarctic Res. Ser. 73, 121–137.
Leventer, A., Dunbar, R.B., 1987. Diatom flux in McMurdo Sound, Antarctica. Mar. Micropaleontol. 12, 49–64.
Leventer, A., Dunbar, R.B., 1988. Recent diatom record of McMurdo Sound, Antarctica: implications for history of sea ice extent. Paleoceanography 3 (3), 259–274.
Leventer, A., Dunbar, R.B., 1996. Factors influencing the distribution of diatoms and other algae in the Ross Sea. J. Geophys. Res. Oceans 101 (C8), 18489–18500.
Leventer, A., Domack, E., Barkoukis, A., McAndrews, B., Murray, J., 2002. Laminations from the Palmer Deep: a diatom-based interpretation. Paleoceanography 17 (3).
Liu, J., Curry, J.A., Martinson, D.G., 2004. Interpretation of recent Antarctic sea ice variability. Geophys. Res. Lett. 31 (2) (n/a).
Mackensen, A., Grobe, H., Kuhn, G., Fu, D., 1990. Benthic foraminiferal assemblages from the eastern Weddell Sea between 68 and 73 °S: distribution, ecology and fossilization potential. Mar. Micropaleontol. 16 (3–4), 241–283.
Majewska, R., Gambi, M.C., Totti, C.M., Pennesi, C., De Stefano, M., 2013. Growth form analysis of epiphytic diatom communities of Terra Nova Bay (Ross Sea, Antarctica). Polar Biol. 36 (1), 73–86.
Majewski, W., Anderson, J.B., 2009. Holocene foraminiferal assemblages from Firth of Tay, Antarctic Peninsula: paleoclimate implications. Mar. Micropaleontol. 73 (3), 135–147.
Majewski, W., Tatur, A., 2009. A new Antarctic foraminiferal species for detecting climate change in sub-Recent glacier-proximal sediments. Antarct. Sci. 21 (5), 439–448.
Majewski, W., Wellner, J.S., Anderson, J.B., 2016. Environmental connotations of benthic foraminiferal assemblages from coastal West Antarctica. Mar. Micropaleontol. 124, 1–15.
Malmgren, B.A., Haq, B.U., 1982. Assessment of quantitative techniques in paleobiogeography. Mar. Micropaleontol. 7 (3), 213–236.
Martinson, D., McKee, D., 2012. Transport of warm upper circumpolar deep water onto the western Antarctic Peninsula continental shelf. Ocean Sci. 8 (4), 433.
Michalchuk, B.R., Anderson, J.B., Wellner, J.S., Manley, P.L., Majewski, W., Bohaty, S., 2009. Holocene climate and glacial history of the northeastern Antarctic Peninsula: the marine sedimentary record from a long SHALDRIL core. Quat. Sci. Rev. 28 (27), 3049–3065.
Milam, R., Anderson, J., 1981. Distribution and ecology of recent benthonic foraminifera and of the Adelie-George-V continental shelf and slope, Antarctica. Mar. Micropaleontol. 6 (3), 297–325.
Milliken, K.T., Anderson, J.B., Wellner, J.S., Bohaty, S.M., Manley, P.L., 2009. High-resolution Holocene climate record from Maxwell Bay, South Shetland Islands, Antarctica. Geol. Soc. Am. Bull. 121 (11/12), 1711–1725.
Morris, E.M., Vaughan, D.G., 2003. Spatial and temporal variation of surface temperature on the Antarctic Peninsula and the limit of viability of ice shelves. In: Antarctic Peninsula Climate Variability: Historical and Paleoenvironmental Perspectives. American Geophysical Union, pp. 61–68.
Mulvaney, R., Abram, N.J., Hindmarsh, R.C., Arrowsmith, C., Fleet, L., Triest, J., Sime, L.C., Alemany, O., Foord, S., 2012. Recent Antarctic Peninsula warming relative to Holocene climate and ice-shelf history. Nature 489 (7414), 141–144.
Murray, J.W., 2001. The niche of benthic foraminifera, critical thresholds and proxies. Mar. Micropaleontol. 41 (1), 1–7.
Murray, J.W., Pudsey, C.J., 2004. Living (stained) and dead foraminifera from the newly ice-free Larsen Ice Shelf, Weddell Sea, Antarctica: ecology and taphonomy. Mar. Micropaleontol. 53 (1), 67–81.
Orsi, A.H., Nowlin, W.D., Whitworth, T., 1993. On the circulation and stratification of the Weddell Gyre. Deep-Sea Res. I Oceanogr. Res. Pap. 40 (1), 169–203.
Parker, W.C., Arnold, A.J., 2003. Quantitative methods of data analysis in foraminiferal ecology. In: Modern Foraminifera. Springer Netherlands, Dordrecht, pp. 71–89.
Parkinson, C., Cavalieri, D., 2012. Antarctic Sea ice variability and trends, 1979-2010. Cryosphere 6 (4), 871.
Pike, J., Allen, C.S., Leventer, A., Stickley, C.E., Pudsey, C.J., 2008. Comparison of contemporary and fossil diatom assemblages from the western Antarctic Peninsula. Mar. Micropaleontol. 67, 274–287.
Pudsey, C.J., Evans, J., 2001. First survey of Antarctic sub–ice shelf sediments reveals mid-Holocene ice shelf retreat. Geology 29 (9), 787–790.
Pudsey, C.J., Murray, J.W., Appleby, P., Evans, J., 2006. Ice shelf history from petrographic and foraminiferal evidence, Northeast Antarctic Peninsula. Quat. Sci. Rev. 25 (17), 2357–2379.
Reynolds, R.W., Smith, T.M., 1994. Improved global sea surface temperature analyses using optimum interpolation. J. Clim. 7 (6), 929–948.
Rignot, E., Casassa, G., Gogineni, P., Krabill, W., Rivera, A., Thomas, R., 2004. Accelerated ice discharge from the Antarctic Peninsula following the collapse of Larsen B ice shelf. Geophys. Res. Lett. 31 (18) (n/a).
Robertson, R., Visbeck, M., Gordon, A.L., Fahrbach, E., 2002. Long-term temperature trends in the deep waters of the Weddell Sea: deep-sea research Part II. Top. Stud. Oceanogr. 49 (21), 4791–4806.
Rott, H., Rack, W., Skvarca, P., De Angelis, H., 2002. Northern Larsen ice shelf, Antarctica: further retreat after collapse. Ann. Glaciol. 34 (1), 277–282.
Scambos, T.A., Bohlander, J., Shuman, C.u., Skvarca, P., 2004. Glacier acceleration and thinning after ice shelf collapse in the Larsen B embayment, Antarctica. Geophys. Res. Lett. 31 (18).
Scherer, R.P., 1994. A new method for the determination of absolute abundance of diatoms and other silt-sized sedimentary particles. J. Paleolimnol. 12 (2), 171–179.
Schmiedl, G., Mackensen, A., Müller, P., 1997. Recent benthic foraminifera from the eastern South Atlantic Ocean: dependence on food supply and water masses. Mar. Micropaleontol. 32 (3), 249–287.
Shevenell, A.E., Kennett, J.P., 2002. Antarctic Holocene climate change: A benthic foraminiferal stable isotope record from Palmer Deep. Paleoceanography 17 (2), 1–12.
Shevenell, A.E., Domack, E.W., Kernan, G.M., 1996. Record of Holocene palaeoclimate change along the Antarctic Peninsula: evidence from glacial marine sediments, Lallemand Fjord. In: Proceedings Papers and Proceedings of the Royal Society of Tasmania 130. pp. 55–64.
Skvarca, P., Rack, W., Rott, H., Donángelo, T.I., 1999. Climatic trend and the retreat and disintegration of ice shelves on the Antarctic Peninsula: an overview. Polar Res. 18 (2), 151–157.
Smith, D.A., Klinck, J.M., 2002. Water properties on the west Antarctic Peninsula continental shelf: a model study of effects of surface fluxes and sea ice. Deep-Sea Res. II Top. Stud. Oceanogr. 49 (21), 4863–4886.
Stammerjohn, S., Massom, R., Rind, D., Martinson, D., 2012. Regions of rapid sea ice change: an inter-hemispheric seasonal comparison. Geophys. Res. Lett. 39 (6).
Stuiver, M., Reimer, P.J., Reimer, R.W., 2017. CALIB 7.1. [WWW program] at. http://calib.org.
Swilo, M., Majewski, W., Minzoni, R.T., Anderson, J.B., 2016. Diatom assemblages from coastal settings of West Antarctica. Mar. Micropaleontol. http://dx.doi.org/10.1016/j.marmicro.2016.04.001.
Szymcek, P., Ishman, S.E., Domack, E.W., Leventer, A., 2007. Holocene oceanographic and climatic variability of the Vega Drift deduced through foraminiferal interpretation. In: US Geological Survey, (2331–1258).
Taylor, F., Whitehead, J., Domack, E., 2001. Holocene paleoclimate change in the Antarctic Peninsula: evidence from the diatom, sedimentary and geochemical record. Mar. Micropaleontol. 41, 25–43.
Tokarczyk, R., 1987. Classification of water masses in the Bransfield Strait and southern part of the Drake Passage using a method of statistical multidimensional analysis. Pol. Polar Res. 4 (08).
Vaughan, D., Doake, C., 1996. Recent atmospheric warming and retreat of ice shelves on the Antarctic Peninsula. Nature 379 (6563), 328.
Vaughan, D.G., Marshall, G.J., Connolley, W.M., Parkinson, C., Mulvaney, R., Hodgson, D.A., King, J.C., Pudsey, C.J., Turner, J., 2003. Recent rapid regional climate warming on the Antarctic Peninsula. Clim. Chang. 60 (3), 243–274.
Villareal, T., Fryxell, G., 1983. Temperature effects on the valve structure of the bipolar diatoms *Thalassiosira antarctica* and *Porosira glacialis*. Polar Biol. 2 (3), 163–169.
Yoon, H.I., Yoo, K.-C., Bak, Y.-S., Lim, H.S., Kim, Y., Lee, J.I., 2010. Late Holocene cyclic glaciomarine sedimentation in a subpolar fjord of the South Shetland Islands, Antarctica, and its paleoceanographic significance: sedimentological, geochemical, and paleontological evidence. Geol. Soc. Am. Bull. 122 (7–8), 1298–1307.
Zielinski, U., Gersonde, R., 1997. Diatom distribution in Southern Ocean surface sediments (Atlantic sector): implications for paleoenvironmental reconstructions. Palaeogeogr. Palaeoclimatol. Palaeoecol. 129 (3), 213–250.